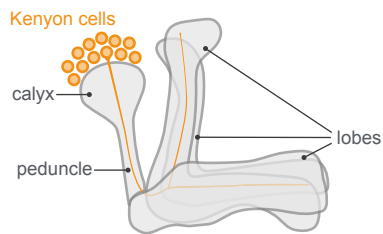


Cell Reports, Volume 36

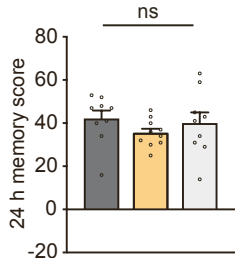
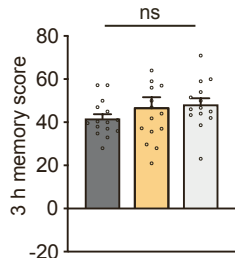
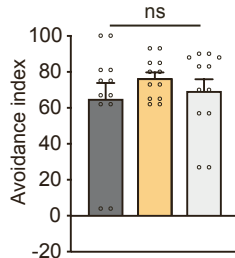
Supplemental information

**Glial glucose fuels the neuronal pentose
phosphate pathway for long-term memory**

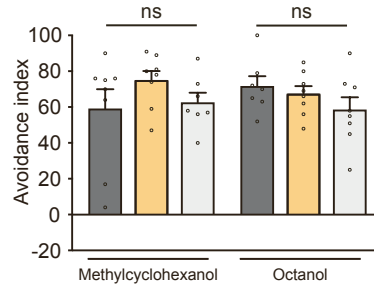
**Eloïse de Treder, Yasmine Rabah, Laure Pasquer, Julia Minatchy, Pierre-Yves
Plaçais, and Thomas Preat**

A

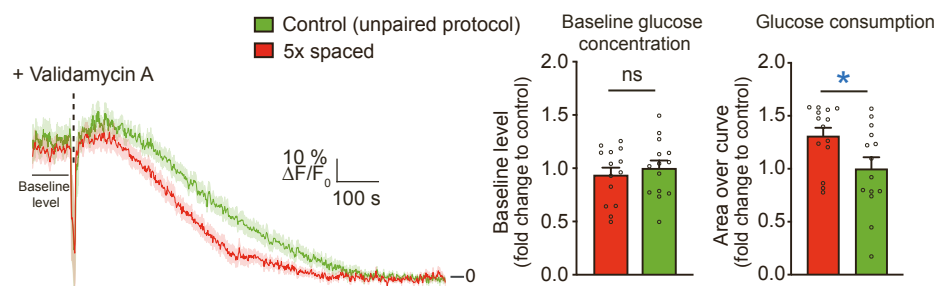
B ■ tub-GAL80^{ts}; VT30559-GAL4/+
 ■ tub-GAL80^{ts}; VT30559-GAL4>UAS-Glut1 RNAi KK108683
 □ +UAS-Glut1 RNAi KK108683

B1 5x spaced, no induction**B2** 1x, induction**B3** Shock avoidance, induction

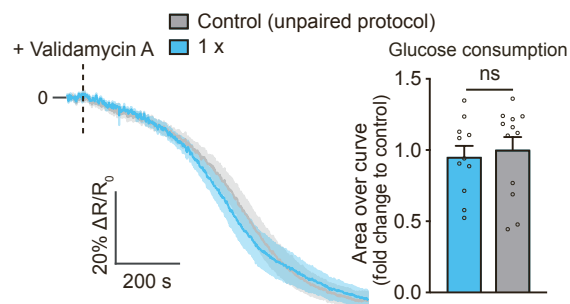
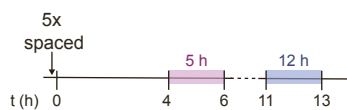
Olfactory acuity, induction

**C**

Glucose imaging in MB neuron somata (low affinity sensor)
 (13F02-LexA>LexAop-iGlucoSnFR), spaced training
 0.5-2 h after training

**D**

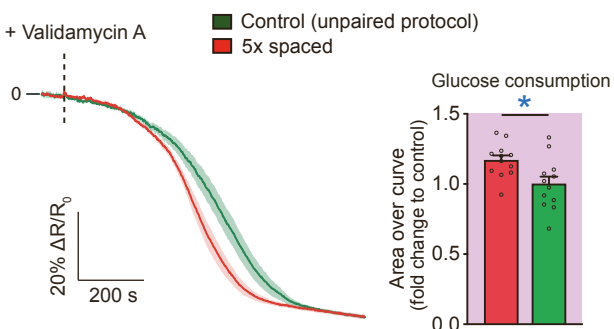
Glucose imaging in MB neuron somata,
 (VT30559-GAL4>UAS-FLII12Pglu-700 μ δ6), 1x training
 0.5-2 h after training

**E**

Glucose imaging in MB neuron somata
 (13F02-LexA>LexAop-FLII12Pglu-700 μ δ6),
 spaced training

E1

5 h after training

**E2**

12 h after training

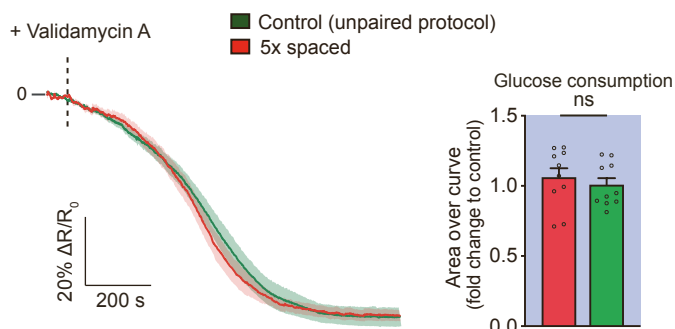
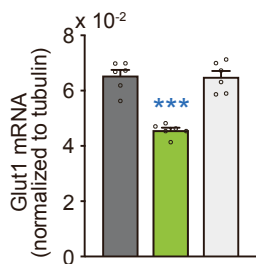


Figure S1. Related to Figure 1.

A. Illustration of mushroom body organization. Kenyon cells (KC) are the intrinsic mushroom body (MB) neurons. MB neuron dendritic processes are bundled into the calyx, where they receive olfactory input from projection neurons. MB neurons then extend parallel axonal fibres bundled in the peduncle. At the distal end of the peduncle, axons show distinct patterns of bifurcation or branching within medial and vertical lobes. MB lobes receive dopaminergic innervation conveying reinforcement signalling (here, through aversive shock stimulation) during olfactory conditioning. B. Control experiments corresponding to Glut1 knock-down in MB neurons. B1. Without induction of the RNAi against Glut1 in MB neurons, LTM in the flies of interest was normal ($n = 9-10$, $F_{2,27} = 0.84$, $P = 0.45$). B2. Glut1 knock-down in MB neurons did not alter 3-h memory after 1 x training ($n = 14-15$, $F_{2,43} = 1.00$, $P = 0.38$). B3. Shock reactivity ($n = 12$, $F_{2,35} = 0.75$, $P = 0.48$) and olfactory acuity (methylcyclohexanol: $n = 7-8$, $F_{2,22} = 1.15$, $P = 0.34$, octanol: $n = 7-8$, $F_{2,22} = 1.3$, $P = 0.29$) were normal in the flies of interest. C. Variations in glucose concentration in the somata of MB neurons expressing the low-affinity iGlucoSnFR glucose sensor were monitored following the application of validamycin A (4 mM), at the time point marked by a dashed line. The injection induced a transient disturbance in the focus, which in turn induced a drop in the recorded signal, as this single-fluorophore sensor is not ratiometric. Data were normalized to the last 150 s of the recording, when a stable floor value was reached corresponding to the unbound state of the sensor. The baseline glucose concentration was then quantified before validamycin A application during the first 90 s of the recording (solid line). No difference in glucose concentration in the somata of MB neurons was observed between flies subjected to 5 x spaced training and flies conditioned with a non-associative spaced unpaired training protocol ($n = 14$, $t_{26} = 0.63$, $P = 0.53$). The glucose concentration in the somata of MB neurons decreased faster following validamycin application in flies after 5 x spaced training as compared to flies conditioned with a non-associative spaced unpaired training protocol ($n = 14$, $t_{26} = 2.30$, $P = 0.030$), similar to what we observed with the high-affinity FRET sensor. D. No difference in glucose consumption was observed between flies subjected to 1 x training or to a non-associative control protocol ($n = 11-12$, $t_{21} = 0.41$, $P = 0.69$), as measured with the glucose FRET sensor. E. Variations in glucose concentration in the somata of MB neurons were monitored following the application of validamycin A (4 mM), at the time point marked by a dashed line. The scheme indicates the time window during which imaging data were collected. E1. Glucose concentration in the somata of MB neurons decreased faster in flies after 5 x spaced training as compared to flies conditioned with a non-associative spaced unpaired training protocol 4 to 6 h after olfactory conditioning ($n = 12$, $t_{22} = 2.65$, $P = 0.015$). E2. Between 11 and 13 h after training, no difference in glucose decrease was observed following validamycin application between flies subjected to 5 x spaced training and a non-associative unpaired protocol ($n = 10$, $t_{18} = 0.65$, $P = 0.52$). Data in C and D were collected between 0.5 and 2 h following the end of the indicated conditioning protocol.

A Quantification of head mRNA extracts

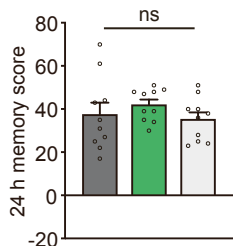
- 54H02-GAL4/+
- 54H02-GAL4>UAS-Glut1 RNAi KK108683
- +/UAS-Glut1 RNAi KK108683



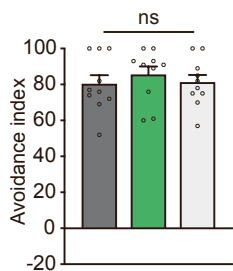
B

- tub-GAL80^{ts}; 54H02-GAL4/+
- tub-GAL80^{ts}; 54H02-GAL4>UAS-Glut1 RNAi GD4552
- +/UAS-Glut1 RNAi GD4552

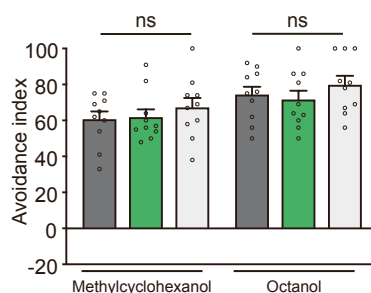
B1 5x spaced, no induction



B2 Shock avoidance, induction



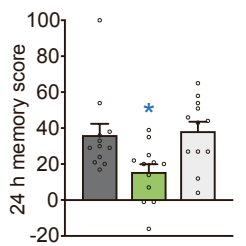
Olfactory acuity, induction



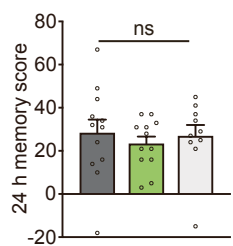
C

- tub-GAL80^{ts}; VT30559-GAL4/+
- tub-GAL80^{ts}; 54H02-GAL4>UAS-Glut1 RNAi KK108683
- +/UAS-Glut1 RNAi KK108683

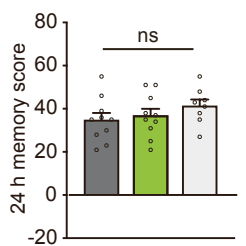
5x spaced, induction



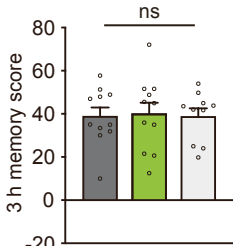
5x massed, induction



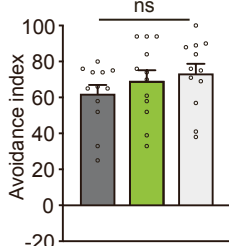
5x spaced, no induction



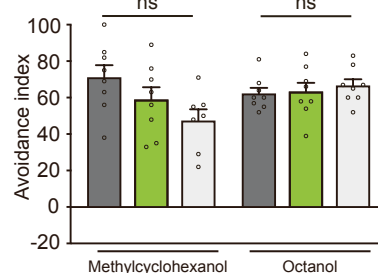
1x, induction



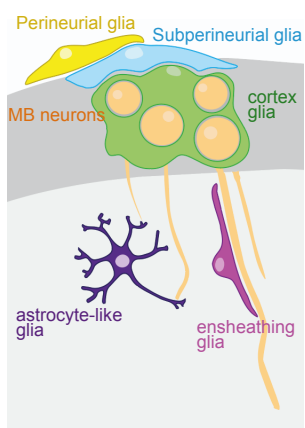
Shock avoidance, induction



Olfactory acuity, induction



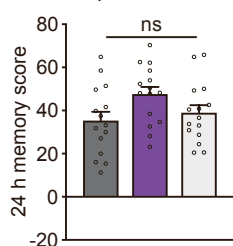
D



E Glut1 KD in adult astrocyte-like glia

- tub-GAL80^{ts}; Alrm-GAL4/+
- tub-GAL80^{ts}; Alrm-GAL4>UAS-Glut1 RNAi KK108683
- +/UAS-Glut1 RNAi KK108683

5x spaced, induction



F Glut1 KD in adult ensheathing glia

- tub-GAL80^{ts}; 56F03-GAL4/+
- tub-GAL80^{ts}; 56F03-GAL4>UAS-Glut1 RNAi KK108683
- +/UAS-Glut1 RNAi KK108683

5x spaced, induction

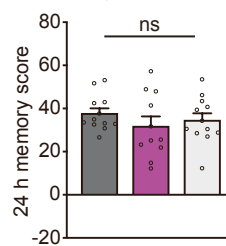
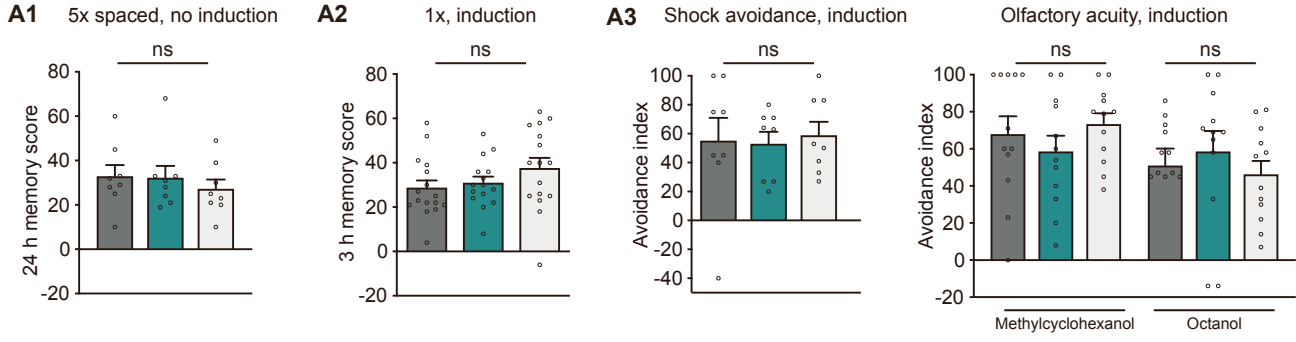


Figure S2. Related to Figure 2.

A. Glut1 knock-down in cortex glia resulted in a significant decrease in overall Glut1 mRNA concentration in the fly brain as measured by RT-qPCR ($N = 3$ independent extracts, $n = 6$ replicates, $F_{2,17} = 36.0$, $P < 0.0001$). B. Control experiments corresponding to Glut1 knock-down (GD4552) in cortex glia. B1. Without RNAi induction, the flies of interest displayed normal LTM ($n = 10$, $F_{2,29} = 0.78$, $P = 0.47$). B2. Shock reactivity ($n = 10$, $F_{2,29} = 0.36$, $P = 0.70$) and olfactory acuity (methylcyclohexanol: $n = 10$, $F_{2,29} = 0.54$, $P = 0.59$, octanol: $n = 10$, $F_{2,29} = 0.72$, $P = 0.49$) were not altered by Glut1 knock-down in cortex glia. C. The whole series of experiments was performed with a second RNAi against Glut1. Knock-down of Glut1 (RNAi KK108683) in adult cortex glia disrupted LTM as compared to the genotypic controls after 5 x spaced training ($n = 12$, $F_{2,35} = 5.11$, $P = 0.012$), but did not affect 24-h memory after 5 x massed training ($n = 10/12$, $F_{2,33} = 0.27$, $P = 0.77$). Without induction of the RNAi, LTM in the flies of interest was normal ($n = 8-10$, $F_{2,27} = 1.05$, $P = 0.37$). 3-h memory after 1 x training was not affected upon Glut1 knock-down ($n = 10/11$, $F_{2,31} = 0.023$, $P = 0.98$). Shock reactivity ($n = 12$, $F_{2,35} = 1.04$, $P = 0.36$) and olfactory acuity (methylcyclohexanol: $n = 7/8$, $F_{2,22} = 3.03$, $P = 0.07$, octanol: $n = 8$, $F_{2,23} = 0.33$, $P = 0.72$) were normal after Glut1 knock-down in cortex glia. D. Subtypes and localization of *Drosophila* glia. Perineurial (yellow) and subperineurial (blue) glia form a chemical and physical barrier for the brain. In the cortical region (dark grey), cortex glia (green) encase cell bodies of neurons (orange). In the neuropile (light grey), astrocyte-like glia (purple) extend processes close to the synapses. Ensheathing glia (pink) processes delimit brain anatomical structures. E. LTM was normal when Glut1 RNAi (KK108683) was expressed in adult astrocyte-like glia using the Alrm-GAL4 driver ($n = 15$, $F_{2,44} = 2.76$, $P = 0.07$). F. LTM was normal when Glut1 RNAi (KK108683) was expressed in adult ensheathing glia using the 56F03-GAL4 driver ($n = 11/12$, $F_{2,34} = 0.75$, $P = 0.48$).

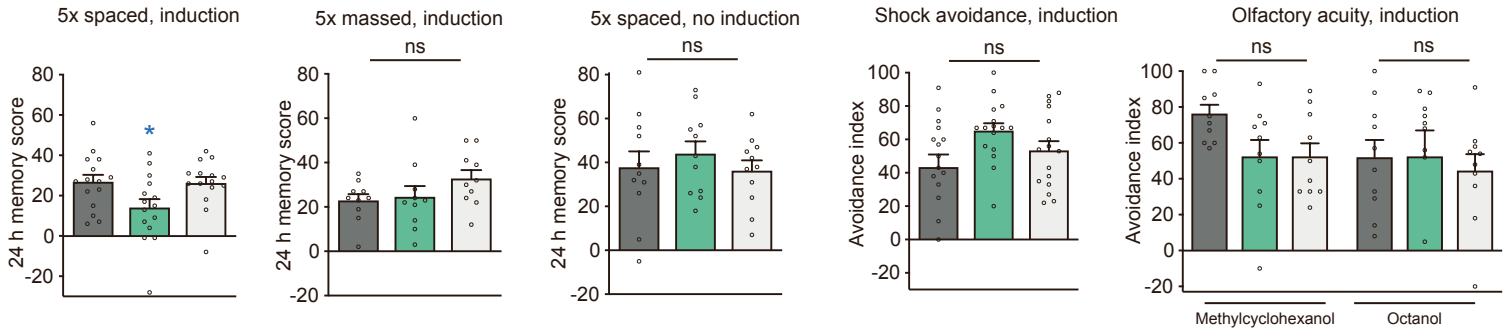
A

- tub-GAL80^{ts}; 54H02-GAL4/+
- tub-GAL80^{ts}; 54H02-GAL4>UAS-nAChR α 7 RNAi JF02570
- +/UAS-nAChR α 7 RNAi JF02570



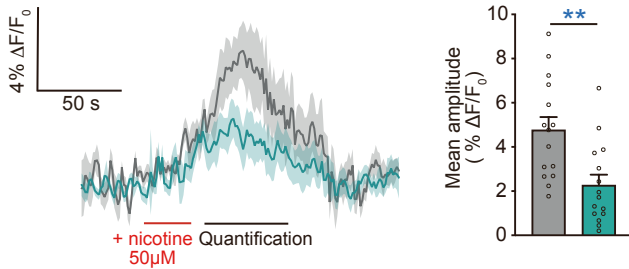
B

- tub-GAL80^{ts}; 54H02-GAL4/+
- tub-GAL80^{ts}; 54H02-GAL4>UAS-nAChR α 7 RNAi KK108471
- +/UAS-nAChR α 7 RNAi KK108471



C Calcium imaging in cortex glia

- tub-GAL80^{ts}; 54H02-GAL4> UAS-GCaMP6f, UAS-Dcr-2
- tub-GAL80^{ts}; 54H02-GAL4> UAS-GCaMP6f, UAS-Dcr-2, UAS-nAChR α 7 RNAi JF02570



D Glucose imaging in cortex glia

- tub-GAL80^{ts}; 54H02-GAL4>UAS-FLII12Pglu-700 μ 66
- tub-GAL80^{ts}; 54H02-GAL4>UAS-FLII12Pglu-700 μ 66; UAS-Glut1 RNAi KK108683

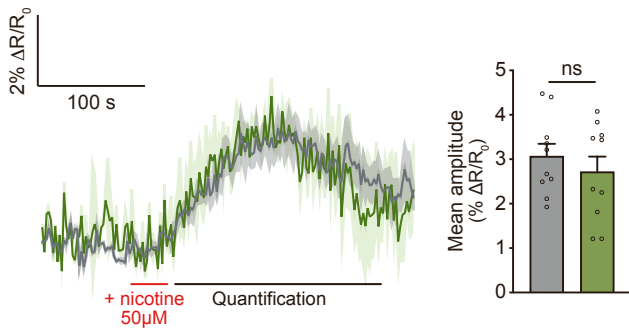
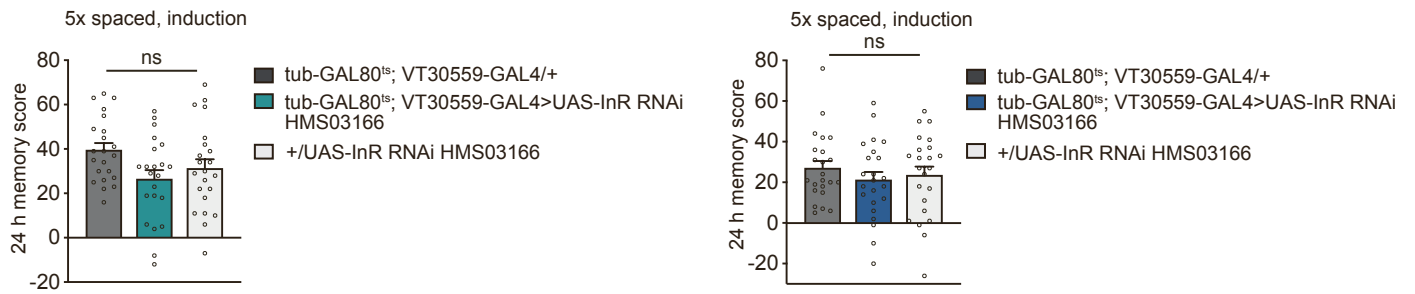
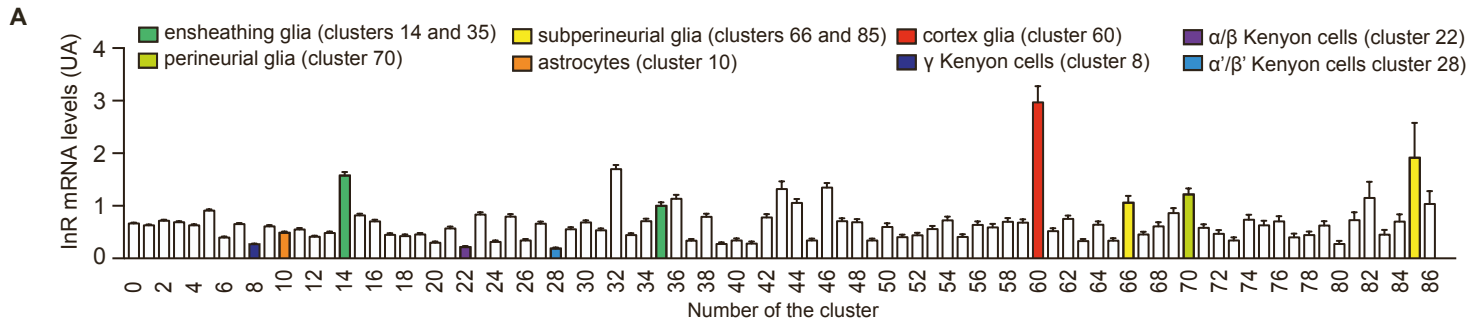
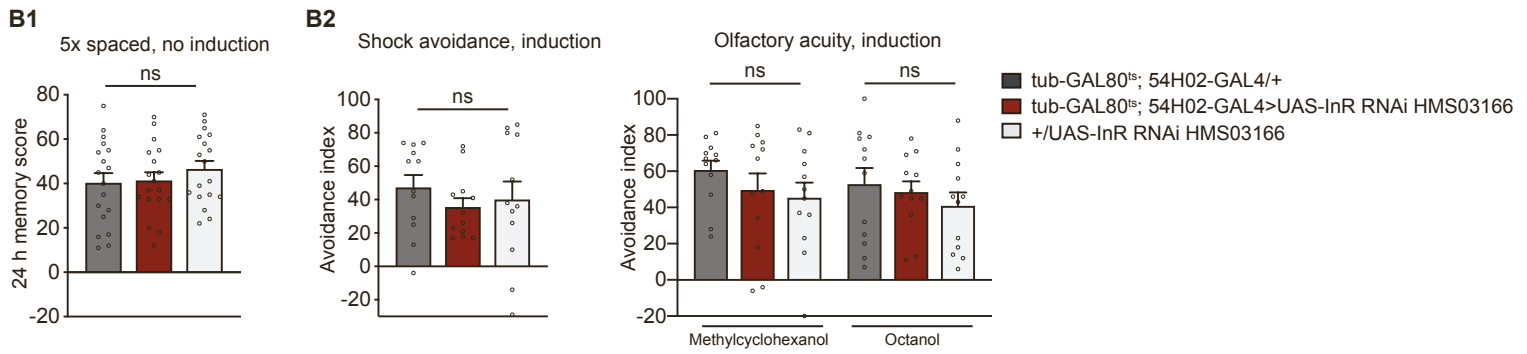


Figure S3. Related to Figure 3.

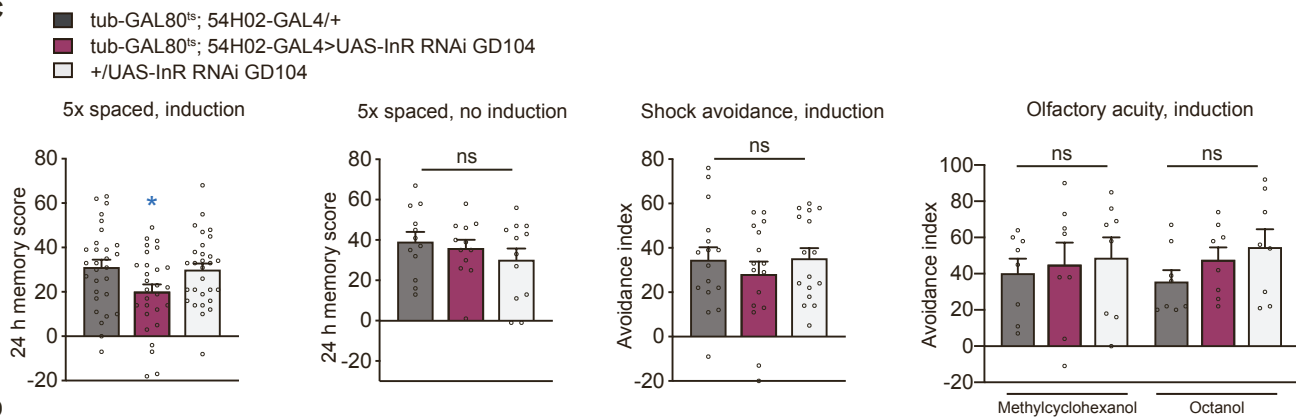
A. Control experiments corresponding to nAChR α 7 knock-down in cortex glia. A1. Without thermal induction of nAChR α 7 JF02570 RNAi expression, no LTM defect was displayed by the flies of interest as compared to the genotypic controls (n = 8, $F_{2,23} = 0.38$, $P = 0.69$). A2. 3-h memory after 1 x training was not affected upon nAChR α 7 knock-down (n = 16, $F_{2,46} = 1.52$, $P = 0.23$). A3. Shock reactivity (n = 8, $F_{2,23} = 0.064$, $P = 0.94$) and olfactory acuity (methylcyclohexanol: n = 12, $F_{2,35} = 0.82$, $P = 0.45$, octanol: n = 12, $F_{2,35} = 0.44$, $P = 0.65$) were not altered by nAChR α 7 knock-down. B. The whole series of experiments was performed with a second RNAi against nAChR α 7. RNAi induction caused impaired LTM (n = 15, $F_{2,44} = 3.76$, $P = 0.031$) while leaving 24-h memory unaffected after 5 x massed training (n = 10, $F_{2,29} = 1.72$, $P = 0.20$). Without RNAi expression, LTM in the flies of interest was normal (n = 11, $F_{2,32} = 0.46$, $P = 0.64$). Shock reactivity (n = 16, $F_{2,47} = 3.09$, $P = 0.055$) and olfactory acuity (methylcyclohexanol: n = 10, $F_{2,29} = 3.36$, $P = 0.05$, octanol: n = 10, $F_{2,29} = 0.15$, $P = 0.86$) were normal after nAChR α 7 knock-down. C. Calcium dynamics in cortex glia were monitored by *In vivo* imaging following nicotine application onto the brain. Dicer-2 (Dcr-2) expression was used to increase the efficiency of RNA interference knock-down of nAChR α 7. Following nicotine perfusion, the induced calcium increase was reduced when nAChR α 7 was knocked-down in cortex glia (n = 15, $t_{28} = 3.32$, $P = 0.0025$). D. The FRET glucose sensor expression was targeted to cortex glia in 54H02-GAL4>UAS-FLII12Pglu-700 μ δ 6 flies. After 30 s of 50 μ M nicotine stimulation (indicated by a red line), the glucose concentration was sustainably increased in cortex glia. Decreasing the expression levels of Glut1 in adult cortex glia had no effect on the nicotine-induced glucose elevation as measured during the 200-s quantification window (black line), starting 10 s after the end of nicotine perfusion (n = 10, $t_{18} = 0.80$, $P = 0.44$).



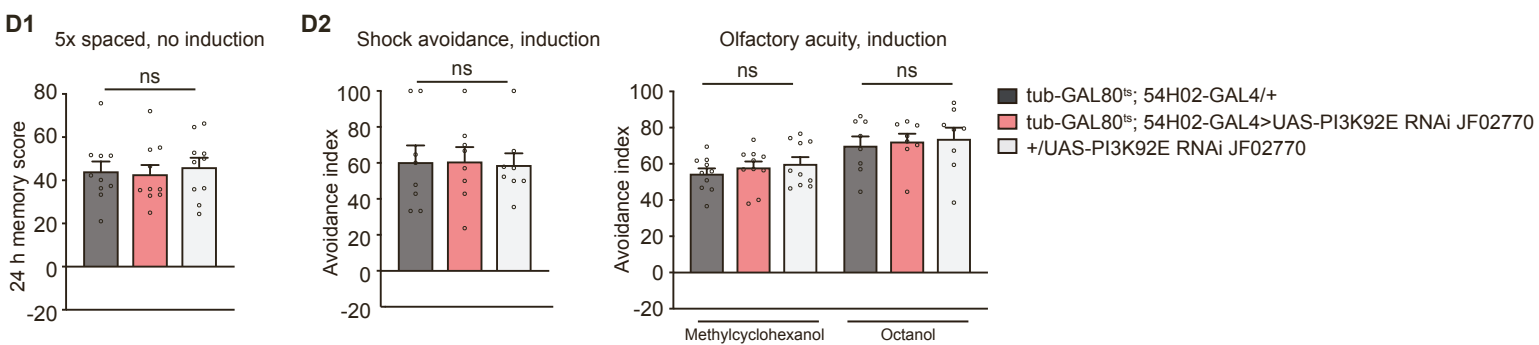
B



C



D



E

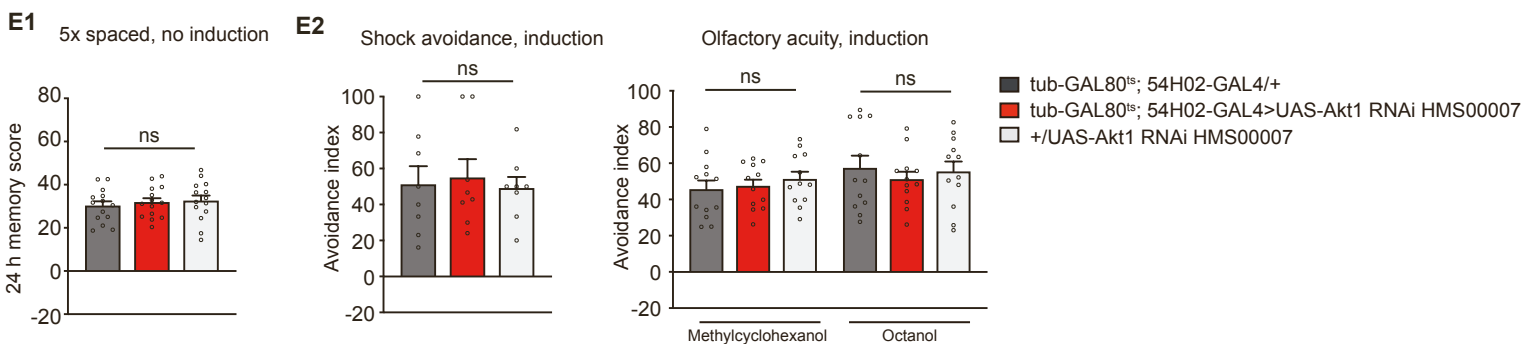


Figure S4. Related to Figure 4.

A. Relative expression of InR in various cell clusters according to published single-cell transcriptomics data (Davie et al., 2018). The number of the cluster in the original study is indicated under each bar, and relevant clusters are displayed in colour and notated. Levels of InR mRNA are higher in glial cells, particularly in cortex glia (cluster 60) as compared to MB neurons (clusters 8, 22, 28). A low level of InR expression in MB neurons is consistent with our behavioural data showing no involvement of the MB neuron InR in LTM. InR knock-down in MB neurons induced at the adult stage in all MB neurons (using the VT30559-GAL4 line) or in α/β MB neurons (using the c739-GAL4 line) did not disrupt LTM (all MB neurons: $n = 22$, $F_{2,65} = 3.05$, $P = 0.054$; α/β MB neurons: $n = 23$, $F_{2,68} = 0.56$, $P = 0.58$). This result is in apparent contradiction to a previous report concluding that insulin signalling is required in MB neurons for LTM formation (Chambers et al., 2015). The conclusion from this study was exclusively drawn from experiments using the constitutive knock-down of InR. Given that insulin signalling in neuroblasts is crucial during development (Chell and Brand, 2010) and that mutants of the insulin receptor substrate *chico* show cell-autonomous developmental defects in MB size and number of neurons (Naganos et al., 2012), it is possible that phenotypes observed with constitutively decreased InR expression were due to subtle developmental defects in MB physiology. Chambers and colleagues also reported that a knock-down of InR at the adult stage impairs LTM, although this result was obtained using a ubiquitous, heat shock inducible driver that includes neuronal and glial cells. Therefore, considering only the experiments performed with inducible tools that are devoid of any possible developmental issues, the published results can be explained by an acute role for InR signalling in cortex glia during LTM formation.

B. Control experiments corresponding to InR knock-down in cortex glia.

B1. In cortex glia, in the absence of thermal induction of the RNAi against InR, LTM in the flies of interest was normal ($n = 18$, $F_{2,53} = 0.69$, $P = 0.51$).

B2. Shock reactivity ($n = 12$, $F_{2,35} = 0.50$, $P = 0.61$) and olfactory acuity (methylcyclohexanol: $n = 12$, $F_{2,35} = 1.00$, $P = 0.38$, octanol: $n = 12$, $F_{2,35} = 0.62$, $P = 0.54$) were normal after InR knock-down.

C. The series of experiments concerning InR knockdown in cortex glia was performed with another RNAi. InR knock-down in cortex glia at the adult stage disrupted LTM ($n = 28-30$, $F_{2,85} = 3.41$, $P = 0.038$). Without RNAi induction, LTM in the flies of interest was normal ($n = 12$, $F_{2,35} = 0.83$, $P = 0.45$). Shock reactivity ($n = 16$, $F_{2,47} = 0.52$, $P = 0.60$) and olfactory acuity (methylcyclohexanol: $n = 8$, $F_{2,23} = 0.67$, $P = 0.49$, octanol: $n = 8$, $F_{2,23} = 1.45$, $P = 0.27$) were normal after InR knock-down.

D. Control experiments corresponding to PI3K92E knock-down in cortex glia.

D1. In cortex glia, in the absence of thermal induction of the RNAi against PI3K92E, LTM in the flies of interest was normal ($n = 10$, $F_{2,29} = 0.13$, $P = 0.87$).

D2. Shock reactivity ($n = 8$, $F_{2,23} = 0.02$, $P = 0.98$) and olfactory acuity (methylcyclohexanol: $n = 10$, $F_{2,29} = 0.61$, $P = 0.55$, octanol: $n = 8$, $F_{2,23} = 0.13$, $P = 0.88$) were normal after PI3K92E knock-down.

E. Control experiments corresponding to Akt1 knock-down in cortex glia.

E1. In cortex glia, in the absence of thermal induction of the RNAi against Akt1, LTM in the flies of interest was normal ($n = 14$, $F_{2,41} = 0.30$, $P = 0.75$).

E2. Shock reactivity ($n = 8$, $F_{2,23} = 0.10$, $P = 0.90$) and olfactory acuity (methylcyclohexanol: $n = 12$, $F_{2,35} = 0.46$, $P = 0.64$, octanol: $n = 12$, $F_{2,35} = 0.31$, $P = 0.73$) were normal after Akt1 knock-down.

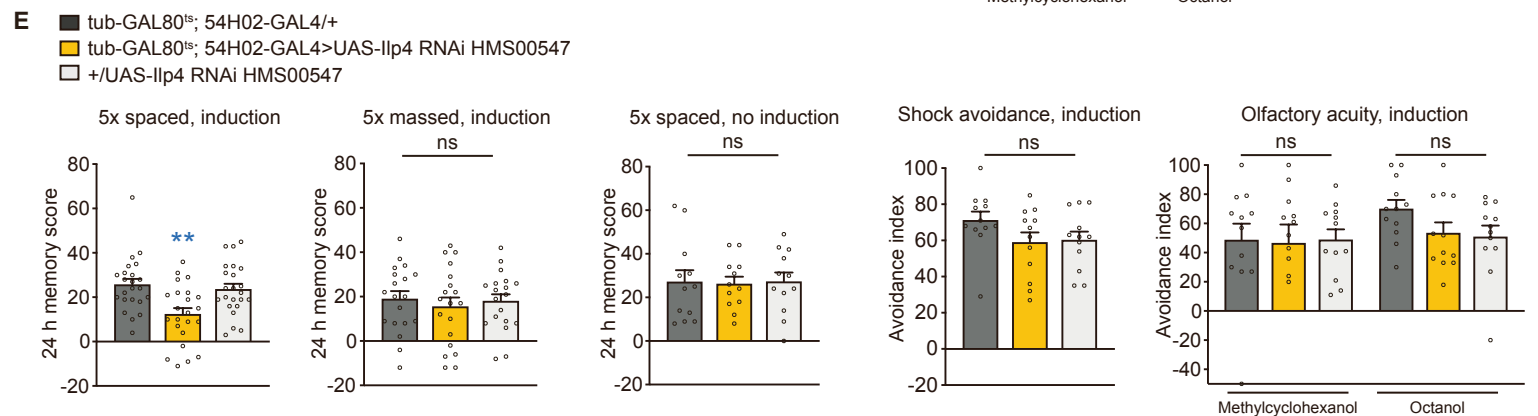
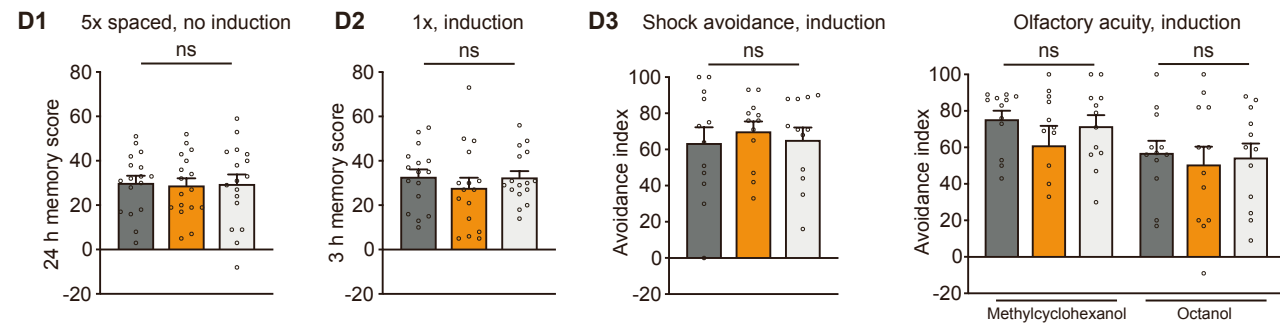
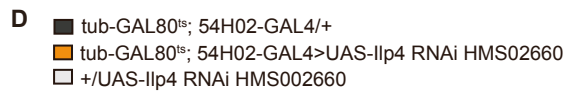
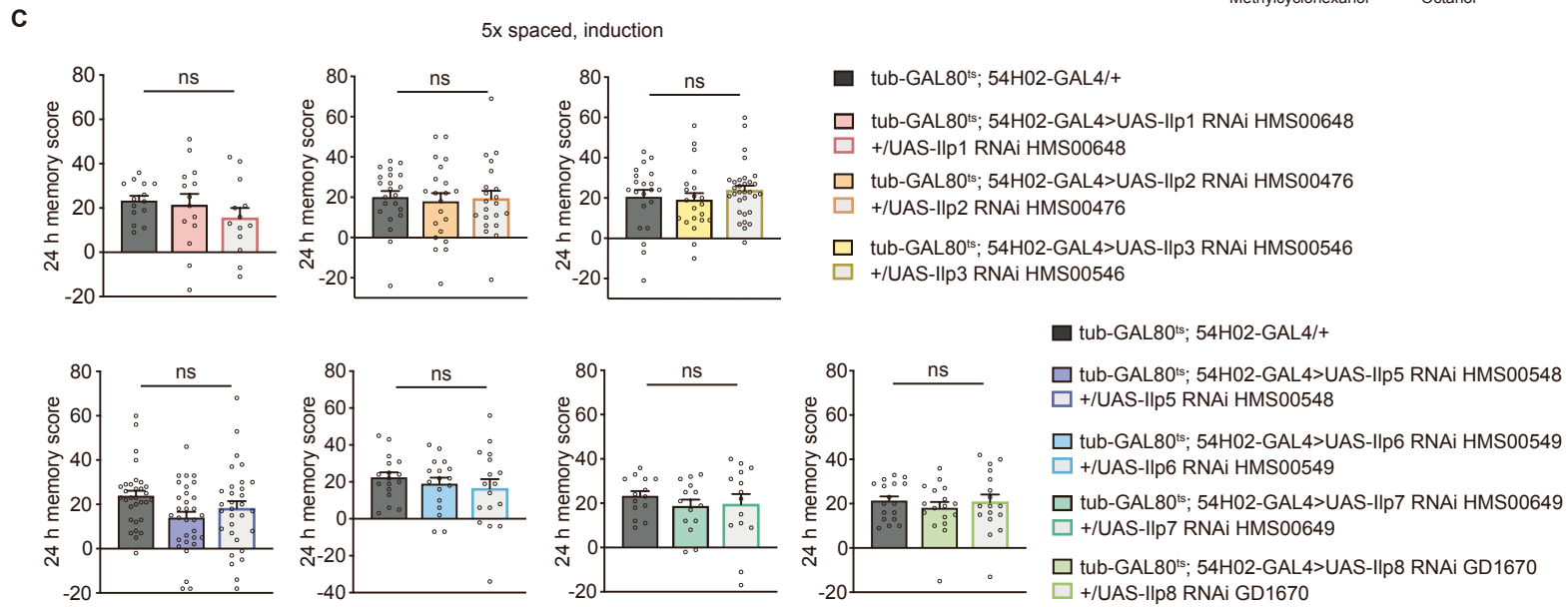
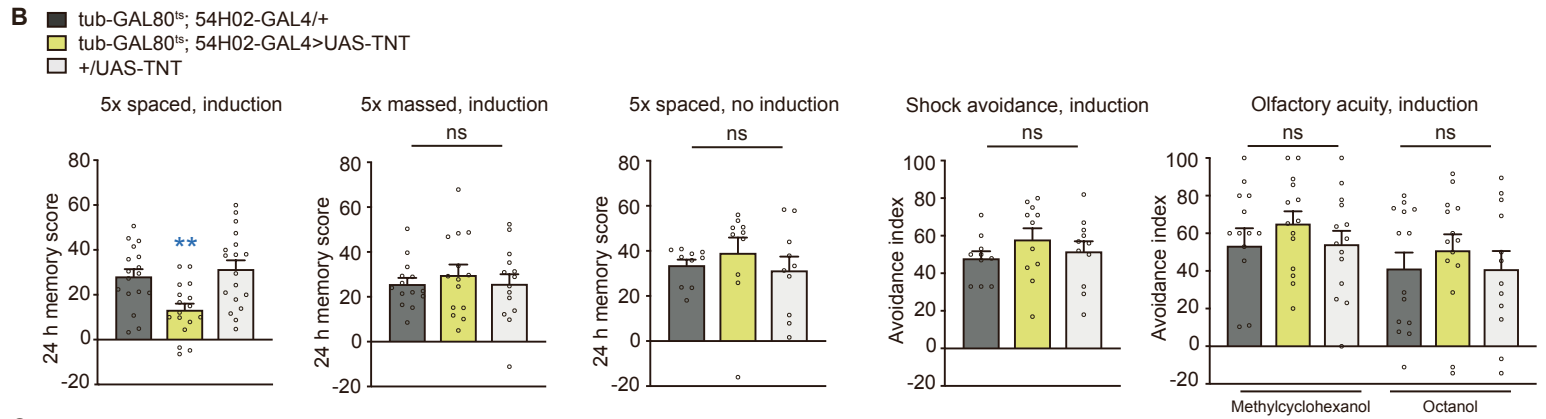
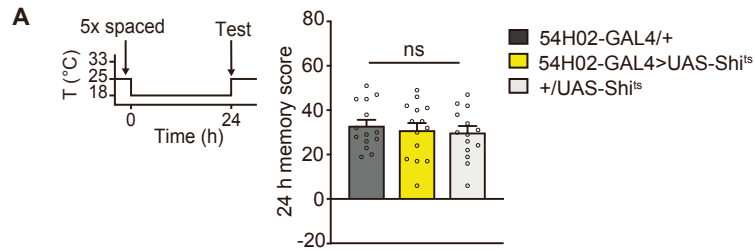
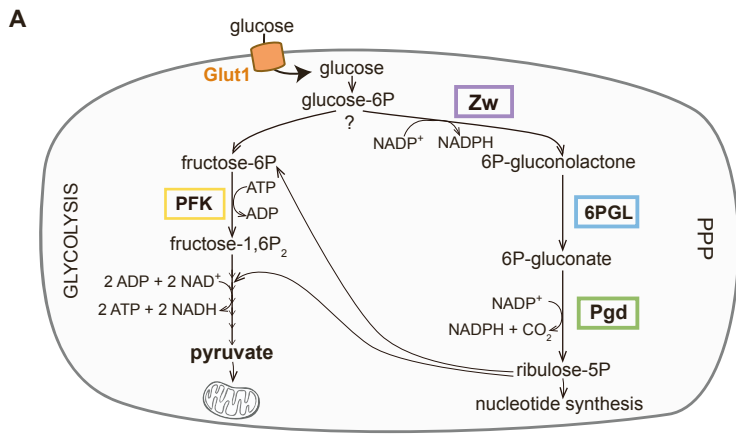
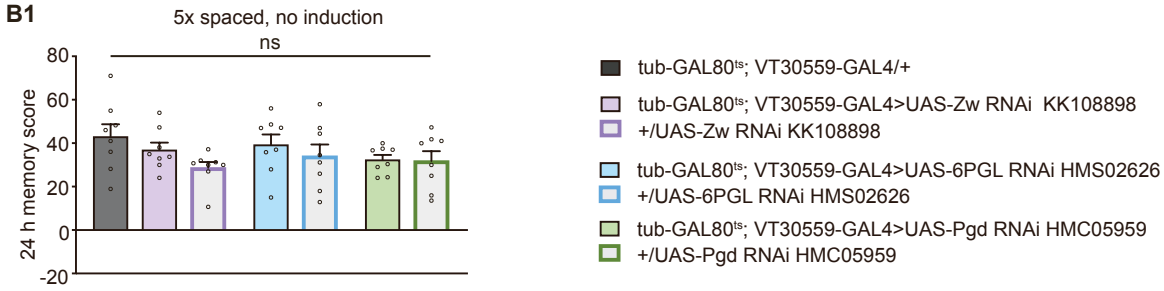


Figure S5. Related to Figure 5.

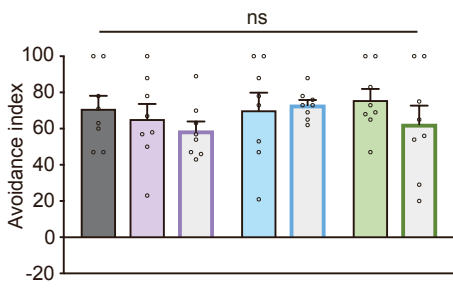
A. Control experiment corresponding to Shi^{ts} expression in cortex glia. The scheme next to the memory graph indicates the time-course of temperature treatments. LTM after spaced training was normal in 54H02-GAL4>UAS- shi^{ts} flies that were not subjected to a restrictive temperature treatment ($n = 14$, $F_{2,41} = 0.25$, $P = 0.78$). B. Blocking vesicular release in adult cortex glia through expression of tetanus toxin (TNT) yielded a significant LTM defect ($n = 17/18$, $F_{2,51} = 7.79$, $P = 0.001$), but did not affect memory tested 24 h after massed training ($n = 14$, $F_{2,39} = 0.30$, $P = 0.74$). Without induction, LTM performance was normal ($n = 10$, $F_{2,29} = 0.52$, $P = 0.60$). Shock reactivity ($n = 10-12$, $F_{2,31} = 0.88$, $P = 0.43$) and olfactory acuity (methylcyclohexanol: $n = 14$, $F_{2,41} = 0.68$, $P = 0.51$, octanol $n = 12-14$, $F_{2,39} = 0.42$, $P = 0.66$) were normal after TNT expression. C. Screen for the role of Ilps in LTM. With the exception of Ilp4 (see Figure 3), knocking down any insulin-like protein in the adult cortex glia did not affect LTM (Ilp1: $n = 13/14$, $F_{2,40} = 0.93$, $P = 0.40$; Ilp2: $n=21/22$, $F_{2,63} = 0.084$, $P = 0.92$; Ilp3: $n=21$, $F_{2,62} = 0.70$, $P = 0.50$; Ilp5: $n = 31$, $F_{2,92} = 2.96$, $P = 0.057$; Ilp6: $n = 17$, $F_{2,50} = 0.57$, $P = 0.57$; Ilp7: $n = 16$, $F_{2,47} = 0.49$, $P = 0.61$; Ilp8: $n = 17$, $F_{2,50} = 0.38$, $P = 0.68$). D. Control experiments corresponding to Ilp4 knock-down in cortex glia. D1. Without thermal induction of Ilp4 RNAi expression, LTM in the flies of interest was normal ($n = 17$, $F_{2,50} = 0.027$, $P = 0.97$). D2. Ilp4 knock-down in the adult cortex glia did not affect memory performance tested at 3 h after 1 x conditioning ($n = 16$, $F_{2,47} = 0.55$, $P = 0.58$). D3. Shock reactivity ($n = 12$, $F_{2,35} = 0.21$, $P = 0.81$) and olfactory acuity (methylcyclohexanol: $n = 12$, $F_{2,35} = 0.91$, $P = 0.41$, octanol: $n = 12$, $F_{2,35} = 0.15$, $P = 0.86$) after Ilp4 knock-down were normal. E. The whole series of experiments was performed with a second RNAi against Ilp4. Ilp4 knock-down in cortex glia exclusively at the adult stage disrupted LTM tested 24 h after 5 x spaced training ($n = 23$, $F_{2,68} = 7.59$, $P = 0.0011$), but did not affect memory tested 24 h after 5 x massed training ($n = 19$, $F_{2,56} = 0.25$, $P = 0.78$). Without Ilp4 RNAi induction, LTM in the flies of interest was normal ($n = 12$, $F_{2,35} = 0.016$, $P = 0.98$). Shock reactivity ($n = 12$, $F_{2,35} = 1.76$, $P = 0.19$) and olfactory acuity (methylcyclohexanol: $n = 12$, $F_{2,35} = 0.016$, $P = 0.98$, octanol: $n = 12$, $F_{2,35} = 2.13$, $P = 0.13$) were normal after Ilp4 knock-down.



B



B2 Shock avoidance, induction



Olfactory acuity, induction

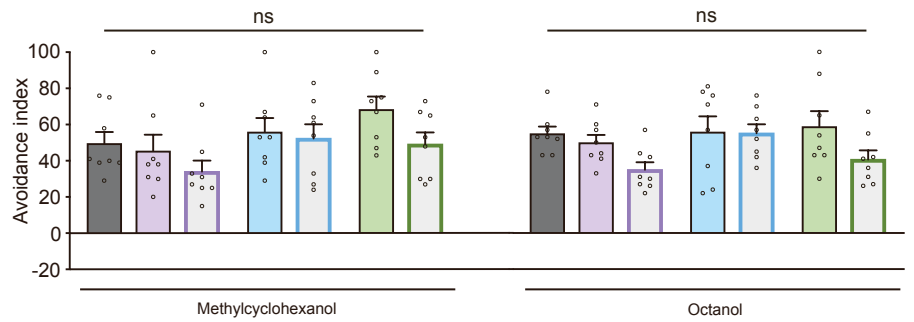


Figure S6. Related to Figure 6.

A. Scheme of the two pathways of cellular glucose catabolism. Glucose is phosphorylated into glucose-6-phosphate (Glucose-6P). Glucose-6P can then be routed into glycolysis, where it is converted into fructose-6-phosphate (Fructose-6P), and in turn phosphorylated into fructose-1,6-bisphosphate (Fructose-1,6P₂) by phosphofructokinase (PFK). Glycolysis produces ATP and pyruvate, which can enter the mitochondrial TCA cycle to fuel electron transport chain and produce ATP. Alternatively, glucose-6P can be directed through the pentose phosphate pathway (PPP) and metabolized into 6-phospho-gluconolactone (6P-gluconolactone) by the glucose-6-phosphate dehydrogenase *Zw*, with the concomitant reduction of NADP⁺ to NADPH. 6P-gluconolactone is then metabolized into 6-phospho-gluconate (6P-gluconate) by 6-phosphogluconolactonase (6PGL). 6P-gluconate is catalysed to ribulose-5-phosphate (ribulose-5P) *via* phosphogluconate dehydrogenase (*Pgd*), accompanied by the reduction of NADP⁺ to NADPH and release of CO₂. Ribulose-5P can be used for generating glycolytic intermediates or for the biosynthesis of nucleotides and thus nucleic acids. These two functions of PPP, anti-oxidant protection and biosynthesis, are not exclusive. B. Control experiments corresponding to the knock-down of the PPP enzymes *Zw*, 6PGL and *Pgd* in MB neurons. B1. Without thermal induction of RNAi expression against *Zw* (RNAi KK108898), 6PGL (RNAi HMS02626) or *Pgd* (RNAi HMC05959), no LTM defect was displayed by the flies of interest as compared to the genotypic controls (n = 8, F_{6,55} = 1.34, P = 0.26). B2. Shock reactivity (n = 8, F_{6,55} = 0.63, P = 0.70) and olfactory acuity (methylcyclohexanol: n = 8, F_{6,55} = 2.05, P = 0.08, octanol: n = 8, F_{6,55} = 2.22, P = 0.06) were not altered by *Zw*, 6PGL or *Pgd* knock-down.